October 6, 2020

The YR Polarimetry - Luminosity Monitor Chapter

Contents

0.1 Lepton and Hadron Polarimetry

Rapid, precise beam polarization measurements will be crucial for meeting the goals of the EIC physics program as the uncertainty in the polarization propagates directly into the uncertainty for relevant observables (asymmetries, etc.). In addition, polarimetry will play an important role in facilitating the setup of the accelerator.

The basic requirements for beam polarimetry are:

- Non-destructive with minimal impact on the beam lifetime
- Systematic uncertainty on the order $\frac{dP}{P} = 1\%$ or better
- Capable of measuring the beam polarization for each bunch in the ring - in particular, the statistical uncertainty of the measurement for a given bunch should be comparable to the systematic uncertainty
- Rapid, quasi-online analysis in order to provide timely feedback for accelerator setup

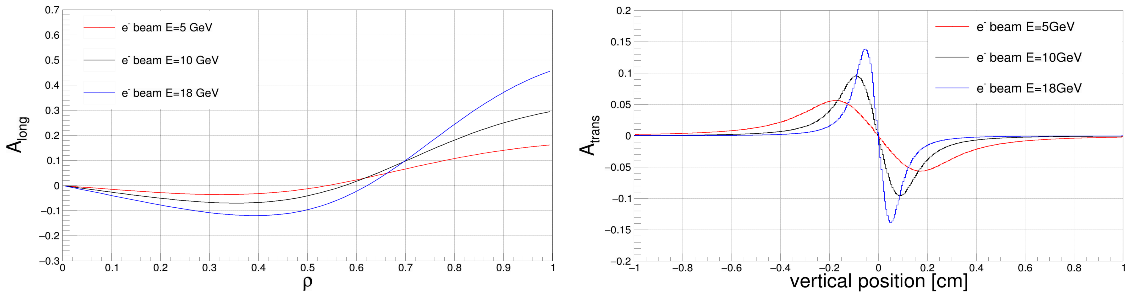

Figure 1: Longitudinal (left) and transverse (right) analyzing powers assuming a 532 nm wavelength laser colliding with an electron beam at 5 GeV, 10 GeV, and 18 GeV. The transverse analyzing power is shown for photons projected 25 m from the collision point and plotted vs. the vertical position.

0.1.1 Electron Polarimetry

The most commonly used technique for measuring electron beam polarization in rings and colliders is Compton polarimetry, in which the polarized electrons scatter from 100% circularly polarized laser photons. The asymmetry from this reaction is measured via the scattered electrons or high energy backscattered photons. A brief review and description of several previous Compton polarimeters can be found in [**?**]. A particular advantage of Compton polarimetry is that it sensitive to both longitudinal and transverse polarization.

The longitudinal analyzing power depends only on the backscattered photon energy and is given by,

$$A_{\text{long}} = \frac{2\pi r_o^2 a}{(d\sigma/d\rho)}(1-\rho(1+a))\left[1-\frac{1}{(1-\rho(1-a))^2}\right], \tag{1}$$

where r_o is the classical electron radius, $a = (1+4\gamma E_{\text{laser}}/m_e)^{-1}$ (with the Lorentz factor $\gamma = E_e/m_e$), ρ is the backscattered photon energy divided by its kinematic maximum, E_γ/E_γ^{max}, and $d\sigma/d\rho$ is the unpolarized Compton cross section. In contrast, the transverse analyzing power depends both on the backscattered photon energy and the azimuthal angle (ϕ) of the photon (with respect to the transverse polarization direction);

$$A_{\text{tran}} = \frac{2\pi r_o^2 a}{(d\sigma/d\rho)}\cos\phi\left[\rho(1-a)\frac{\sqrt{4a\rho(1-\rho)}}{(1-\rho(1-a))}\right]. \tag{2}$$

This azimuthal dependence of the asymmetry results in an "up-down" asymmetry (assuming vertically polarized electrons) and requires a detector with spatial sensitivity. Both the longitudinal and transverse analyzing powers are shown in Fig. 4.

Plans for electron polarimetry at EIC include a Compton polarimeter at IP 12, where the electron beam is primarily vertically polarized. A Compton polarimeter near the primary detector in the vicinity of IP 6, where the beam will be a mix of longitudinal and transverse polarization, is also under investigation; since that region of the ring is extremely crowded, care must be taken in the assessment of whether a polarimeter can be accommodated. A

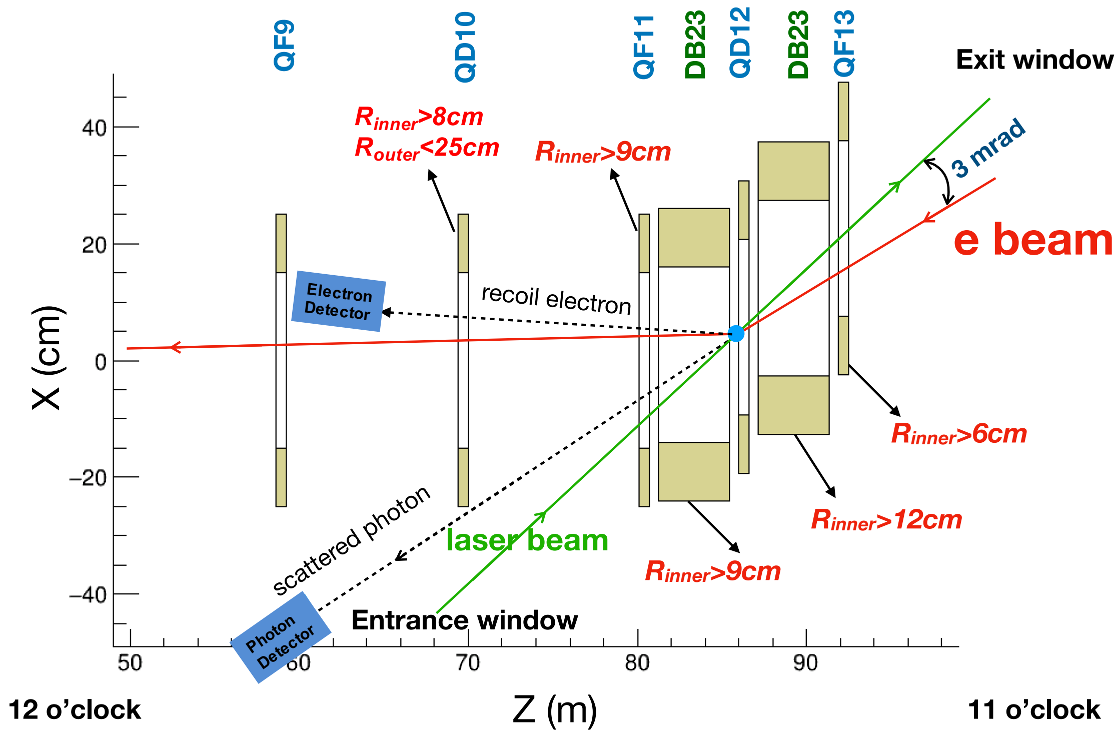

Figure 2: Layout of the Compton polarimeter at IP 12. In this figure the electron beam travels from right to left - the laser beam collides with the electrons just downstream of QD12. The dipole just downstream of the collision (DB12) steers the unscattered electrons allowing detection of the backscattered photons about 25 m downstream of the collision. DB12 also momentum-analyzes the scattered electrons, facilitating use of a position sensitive electron detector downstream of QD10. Also noted in the figure are constraints on required apertures of the magnets needed to allow transport of the laser beam, backscattered photons, and scattered electrons.

schematic of the placement of the Compton polarimeter at IP 12 is shown in Fig. 2.

As noted above, a key requirement of the Compton polarimeter is the ability to make polarization measurements for an individual bunch. The measurement time to achieve a statistical precision dP/P is given by a combination of the luminosity, Compton cross section, and analyzing power:

$$t_{meth} = \left(\mathcal{L} \, \sigma_{\text{Compton}} \, P_e^2 P_\gamma^2 \left(\frac{dP_e}{P_e} \right)^2 \, \text{A}_{\text{eff}}^2 \right)^{-1}. \tag{3}$$

The effective Compton analyzing power, A_{eff}, depends on the measurement technique; in order of increasing effective analyzing power, these are integrated, energy-weighted integrated, and differential. For measurement time estimates here, we will use the smallest analyzing power (i.e., integrated) to be conservative.

Nominal electron beam parameters at IP 12 are provided in Table 1. Of particular note is the relatively short bunch lifetime at 18 GeV. Table 2 shows the average transverse analyzing power, luminosity, and time required to make a 1% (statistics) measurement of the beam polarization for an individual bunch, assuming a single Compton-scattered event per crossing. The constraint of having a single event per crossing is related to the need to make a position sensitive measurement at the photon and electron detectors. Note that even with this constraint, the measurement times are relatively short and, in particular, shorter than the bunch lifetime in the ring.

beam property	5 GeV	10 GeV	18 GeV
Bunch frequency	99 MHz	99 MHz	24.75 MHz
Beam size (x)	390 μm	470 μm	434 μm
Beam size (y)	390 μm	250 μm	332 μm
Pulse width (RMS)	63.3 ps	63.3 ps	30 ps
Intensity (avg.)	2.5 A	2.5 A	0.227 A
Bunch lifetime	>30 min	>30 min	6 min

Table 1: Beam parameters at IP12 for the EIC nominal electron beam energies.

beam energy [GeV]	σ_{unpol} [barn]	$\langle A_\gamma \rangle$	t_γ[s]	$\langle A_e \rangle$	t_e[s]	L[1/(barn·s)]
5	0.569	0.031	184	0.029	210	1.37E+05
10	0.503	0.051	68	0.050	72	1.55E+05
18	0.432	0.072	34	0.075	31	1.81E+05

Table 2: Asymmetries, measurement times needed for a 1% statistical measurement for one bunch and needed luminosities for three different beam energies for a 532 nm laser.

Even for a single electron bunch (circulating through the ring at a frequency of ≈75 kHz), the luminosities provided in Table 2 can be readily achieved using a single-pass, pulsed laser. Since the electron beam frequency varies with energy, it would be useful to have a laser with variable pulse frequency. A laser system based on the gain-switched diode lasers used in the injector at Jefferson Lab [**?**] would provide both the power and flexible pulse frequency desired. Such a system would make use of a gain-switched diode laser at 1064 nm, amplified to high average power (10-20 W) via a fiber amplifier, and then frequency doubled to 532 nm using a PPLN or LBO crystal. The repetition rate is set by the applied RF frequency to the gain-switched seed laser.

A laser system based on the gain-switched diode lasers used in the injector at Jefferson Lab [**?**] can provide all of the requirements noted above. The proposed system will make use of a gain-switched diode laser at 1064 nm, amplified to high average power (10-20 W) via a fiber amplifier, and then frequency doubled to 532 nm using a PPLN or LBO crystal. The repetition rate of the laser is dictated by an applied RF signal and can be readily varied. In addition to the laser system itself, a system to set up and measure the laser

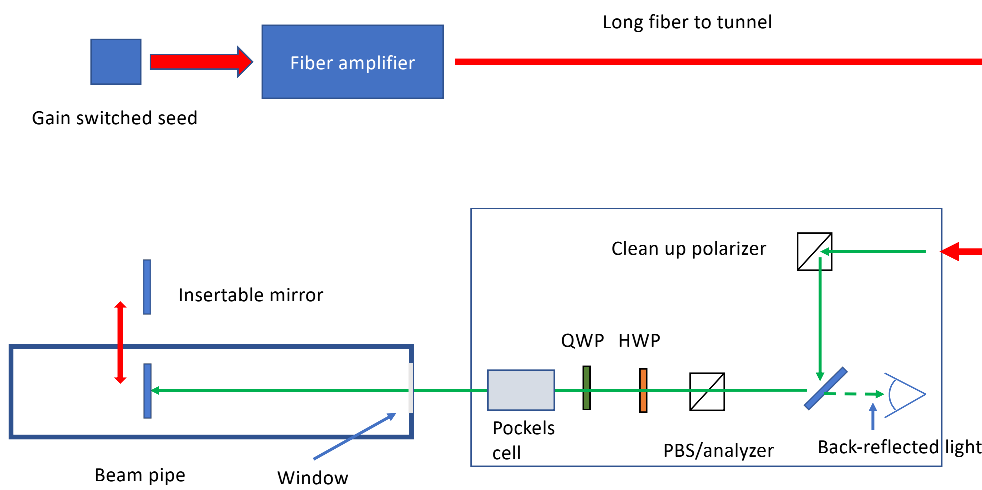

Figure 3: Layout of the Compton polarimeter laser system, including diagnostics to accurately determine the laser polarization at the interaction point.

polarization at the interaction point is required. Determination of the laser polarization in the beamline vacuum is non-trivial due to possible birefringence of the beamline window under mechanical and vacuum stress. We will employ a technique similar to that used at Jefferson Lab [?, ?] that makes use of optical reversibility theorems to determine the laser polarization inside the vacuum using light reflected backwards through the incident laser transport system. This polarization monitoring and setup system will require a remotely insertable mirror in the beamline vacuum so will need to be considered in the beamline design. A schematic of the proposed laser system is shown in Fig. 3.

The detector requirements for the EIC Compton polarimeters are dictated by the requirement to be able to measure the transverse and longitudinal polarization simultaneously. For longitudinal polarization, this means the detectors will require sensitivity to the backscattered photon and scattered electron energy. The photon detector can make use of a fast calorimeter, while the electron detector can take advantage of the dispersion introduced by the dipole after the collision point to infer the scattered electron energy from a detector with position sensitivity in the horizontal direction.

To measure transverse polarization, position sensitive detectors are required to measure the up-down asymmetry. This is particularly challenging given the very small backscattered photon cone at the highest EIC beam energy. At HERA, the vertical position of the backscattered photon was inferred via shower-sharing between the optically isolated segments of a calorimeter [?]. Calibration of the non-linear transformation between the true vertical position and the energy-asymmetry in the calorimeter was a significant source of uncertainty. The proposed detector for the EIC Compton will measure the vertical position directly via segmented strip detectors, avoiding the calibration issues faced at HERA.

The transverse Compton analyzing power vs. position at the detector for the backscattered

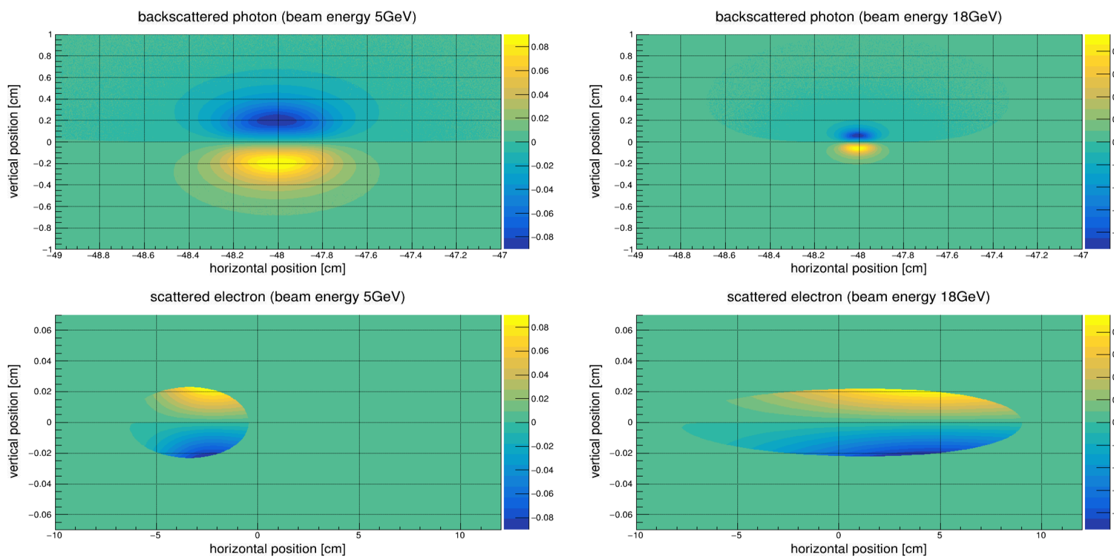

Figure 4: Compton (transverse) analyzing power at the nominal photon and electron detector positions for the IP 12 polarimeter.

photons and scattered electrons at 5 and 18 GeV is shown in Fig. 4. The backscattered photon cone will be largest at the lowest energy (5 GeV) - this will determine the required size of the detector. The distribution at 18 GeV, where the cone is the smallest, sets the requirements for the detector segmentation. Note that the scattered electrons are significantly more focused than the photons. Monte Carlo studies indicate that the transverse polarization can be reliably extracted at 18 GeV with a vertical detector segmentation of 100 μm for the photon detector and 25 μm for the electron detector. The detector size should be at least 16 x 16 mm^2 for the photons and 10 cm x 1 mm for the scattered electrons. The horizontal segmentation for the electron detector can be much more coarse due to the large horizontal dispersion introduced by the dipole.

Diamond strip detectors are a feasible solution for both the photon and electron detectors. Diamond detectors are extremely radiation hard and are fast enough to have response times sufficient to resolve the minimum bunch spacing (10 ns) at EIC. Tests of CVD diamond with specialized electronics have shown pulse widths on the order of 8 ns [**?**]. For the photon detector, about 1 radiation length of lead will be placed in front of the strip detectors to convert the backscattered photons. As an alternative to diamond detectors, HVMAPS detectors are also under consideration. The radiation hardness and time response of HVMAPS will need to be assessed to determine their suitability for this application.

As noted earlier, the photon detector will also require a calorimeter to be sensitive to longitudinal components of the electron polarization. Only modest energy resolution is needed; radiation hardness and time response are more important requirements for this detector - a tungsten powder/scintillating fiber calorimeter would meet these requirements.

Backgrounds are an important consideration for Compton polarimetry as well. The primary processes of interest are Bremsstrahlung and synchrotron radiation. Monte Carlo studies have shown that the contribution from Bremsstrahlung should be small for a beamline vacuum of 10^{-9} Torr. Synchrotron radiation, on the other hand, will be a significant concern. Careful design of the exit window for the backscattered photons will be required to mitigate backgrounds due to synchrotron. The electron detector is not in the direct synchrotron fan, but significant power can be deposited in the detector from one-bounce photons. This can be mitigated by incorporating tips or a special antechamber in the beampipe between the Compton IP and the detector [**?**]. The electron detector will also be subject to power deposited in the planned Roman Pot housing due to the beam Wakefield. Preliminary simulations indicate the Wakefield power should not be large enough to cause problems, but this will need to be considered in the detailed Roman Pot design.

In addition to measurements in the EIC electron ring, it is important to be able to determine the electron beam polarization in or just after the Rapid Cycling Synchrotron (RCS) in order to facilitate machine setup and troubleshoot possible issues with the electron beam polarization. In the RCS, electron bunches of approximately 10 nC are accelerated from 400 MeV to the nominal beam energy (5, 10, or 18 GeV) in about 100 ms. These bunches are then injected into the EIC electron ring at 1 Hz. The short amount of time each bunch spends in the RCS, combined with the large changes in energy (and hence polarimeter analyzing power and/or acceptance) make non-invasive polarization measurements, in which the the RCS operates in a mode completely transparent to beam operations, essentially impossible. However, there are at least two options for making intermittent, invasive polarization measurements.

The first, and perhaps simplest from a polarimetry perspective, would be to operate the RCS in a so-called "flat-top" mode [**?**]. In this case, an electron bunch in the RCS is accelerated to its full or some intermediate energy, and then stored in the RCS at that energy while a polarization measurement is made. In this scenario, a Compton polarimeter similar to that described above could be installed in one of the straight sections of the RCS. The measurement times would be equivalent to those noted in Table 2 (since those are for a single stored bunch), i.e., on the order of a few minutes.

Another option would be to make polarization measurements in the transfer line from the RCS to the EIC electron ring. In this case, one could only make polarization measurements averaged over several bunches. In addition, the measurement would be much more time consuming due to the low average beam current ($\approx$ 10 nA) since the 10 nC bunches are extracted at 1 Hz.

The measurement time at 10 nA using a Compton polarimeter similar to the one planned for IP12 would take on the order many days. The IP12 Compton limits the number of interactions to an average of one per crossing to be able to count and resolve the position of the backscattered photons. A position sensitive detector that could be operated in integrating mode, would allow more rapid measurements. However, the required position resolution (25-100 μm) would be very challenging for a detector operating in integrating mode.

An alternative to Compton polarimetry would be the use of Møller polarimetry. Møller polarimeters can be used to measure both longitudinal and transverse polarization and can

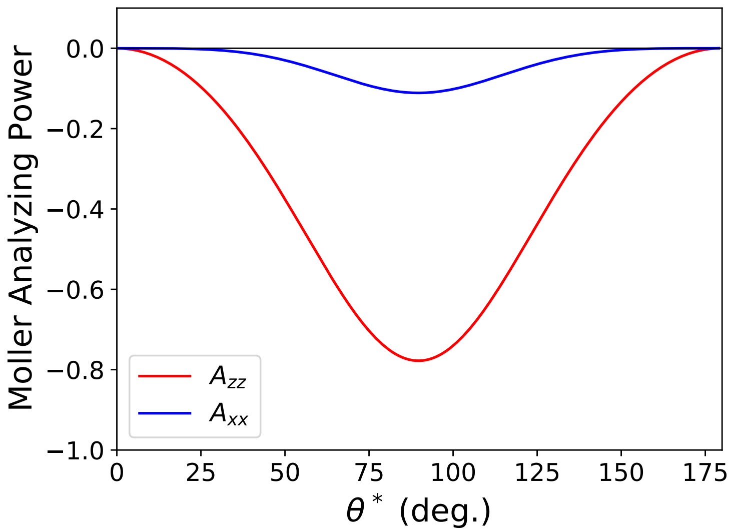

Figure 5: Analyzing power for longitudinally polarized beam and target electrons (A_{zz}) and transversely polarized beam and target electrons (A_{xx}) vs. center of mass scattering angle, θ^*. The magnitude for both is largest at θ^* = 90 degrees; $A_{ZZ} = -7/9$ and A_{XX}=-1/9.

make measurements quickly at relatively low currents. The longitudinal and transverse Møller analyzing powers are shown in Fig. 5 and are given by,

$$A_{ZZ} = -\frac{\sin^2\theta^*(7+\cos^2\theta^*)}{(3+\cos^2\theta^*)^2}, \tag{4}$$

$$A_{XX} = -\frac{\sin^4\theta^*}{(3+\cos^2\theta^*)^2}, \tag{5}$$

where A_{ZZ} is the analyzing power for longitudinally polarized beam and target electrons, A_{XX} for horizontally polarized beam and target electrons, and θ^* is the center-of-mass scattering angle. Note that $A_{YY} = -A_{XX}$. The magnitude of the analyzing power is maximized in both cases at $\theta^* = 90$ degrees, where $|A_{ZZ}| = 7/9$ and $|A_{XX}| = 1/9$.

Møller polarimeters at Jefferson Lab can make (longitudinal) polarization measurements with a statistical precision of 1% at average beam currents of 1 μA with a 4 μm iron foil target in about 15 minutes. Electrons from the RCS will be transversely polarized, and the analyzing power will be a factor of 7 smaller, which implies a factor of 50 increase in measurement time for the same precision. This smaller analyzing power combined with the low average beam current results in very long measurement times. These long measurements times can be partially mitigated through the use of thicker target foils. Even then, the measurements still take a significant amount of time - 1.5 hours for a 10% measurement of the polarization using a 30 μm target. While target foil thicknesses of 10-30 μm have routinely been employed in Møller polarimeters, it is possible that even thicker targets (perhaps a factor of 10 thicker) could also be used, reducing the measurement time

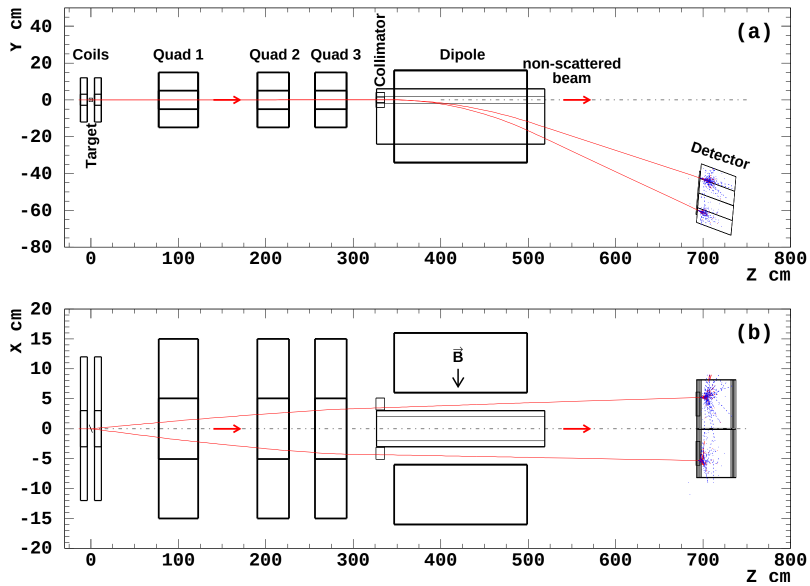

Figure 6: Layout of the Møller polarimeter in experimental Hall A at Jefferson Lab.

further. The maximum useful target thickness would need to be investigated.

A key drawback of Møller polarimetry is that the solid foil targets are destructive to the beam, so cannot be carried out at the same time as normal beam operations. An additional complication is the requirement for a magneto-optical system to steer the Møller electrons to a detector system. In the experimental Hall A at Jefferson Lab, the Møller spectrometer employs several quadrupoles of modest length and aperture, combined with a dipole to deflect the Møller electrons into the detector system (see Fig. 6). The whole system occupies about 7 m of space along the beamline, but the space used by the quadrupoles can also be used for beam transport during normal operations (i.e., when Møller measurements are not underway).

The preferred choice for polarimetry at the RCS is a Compton polarimeter in the RCS ring, with measurements taking place during "flat-top" mode operation. However, if this "flat-top" mode is not practical, then a Møller polarimeter in the RCS transfer line could serve as a reasonable fallback, albeit with reduced precision and a larger impact on the beamline design.

0.1.2 Hadron Polarimetry

Hadron polarimetry has been successfully performed on RHIC polarized proton beams for nearly two decades. Through continual development a systematic uncertainty $\sigma_P^{\text{syst}}/P < 1.5\%$ [**?**] was achieved for the most recent RHIC polarized proton run. After improving data analysis, systematic uncertainties in measurement of the beam profile averaged polarization were reduced to $\sigma_P^{\text{syst}}/P \lesssim 0.5\%$ [**?**]. As the only hadron polarimeter system at a high energy collider it is the natural starting point for hadron polarimetry at the EIC.

Hadron polarization is typically measured via a transverse single spin left right asymmetry: $\epsilon = A_N P$. Unlike for polarized leptons, the proportionality constant is not precisely known from theory. The solution at RHIC employs an absolute polarimeter with a polarized atomic hydrogen jet target (HJET) [**?**], illustrated in Fig. 7. The hydrogen polarization vector is alternated between vertically up and down. The RHIC beam also has bunches with up and down polarization states. By averaging over the beam states the asymmetry with respect to the target polarization may be measured, and vice versa:

$$\epsilon_{\text{target}} = A_N P_{\text{target}} \quad \epsilon_{\text{beam}} = A_N P_{\text{beam}} \; . \tag{6}$$

The target polarization is precisely measured with a Breit-Rabi polarimeter. Combined with the measured asymmetries the beam polarization is determined:

$$P_{\text{beam}} = \frac{\epsilon_{\text{beam}}}{\epsilon_{\text{target}}} P_{\text{target}} \; . \tag{7}$$

The absolute polarization measurement is independent of the details of A_N.

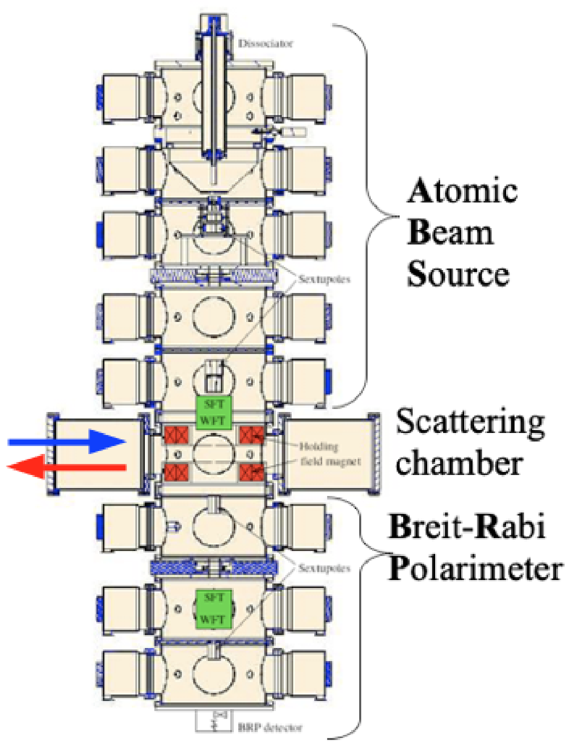

Figure 7: The RHIC polarized hydrogen jet polarimeter. The atomic beam source at the top passes polarized hydrogen across the beams (blue and read arrows) in the scattering chamber, with detectors left and right of the beams. The atomic hydrogen polarization is measured by the Breit-Rabi polarimeter at bottom.

Even though, the diffuse nature of the polarized jet target provides only a relatively low rate of interactions, continuous operation during the store resulted in statistical precision of the polarization measurement of about $\sigma_P^{\text{stat}} \sim 2\%$ per 8–hour RHIC fill (in Run 17). These measurements, however, are not sensitive to the inevitable decay of beam polarization throughout a fill. Also, the jet target is wider than the beam and measures only the average polarization across the beam. The beam polarization is larger at the center than the edges transversely; the polarization of colliding beams differs from the average polarization due to this effect [**?**]. The polarimeters must measure this transverse polarization profile to provide correct polarizations for use by collider experiments.

At RHIC the required finer grained polarization details are provided by the proton-carbon (pC) relative polarimeter, illustrated in Fig. 8. A thin carbon ribbon target is passed across the beam and scattered carbon nuclei are measured in detectors arrayed around the beam. The dense target provides a high interaction rate, allowing an asymmetry measurement with a few per cent statistical precision in less than 30 seconds. Such measurements are made periodically throughout a RHIC fill, providing a measurement of the beam polarization decay. The ribbon target is narrower than the beam; thus it is able to measure asymmetry as a function of position across the beam and determine the transverse polarization profile. The absolute polarization scale of the pC polarimeter is set by normalizing an ensemble of pC measurements to the results from the Hjet polarimeter for the corresponding RHIC fills.

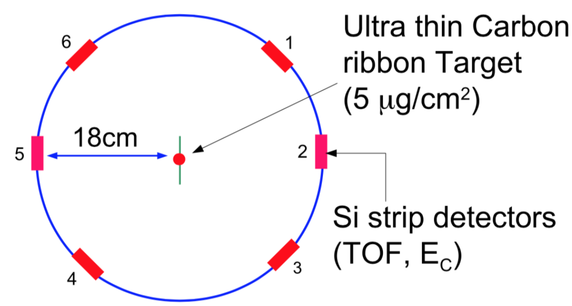

Figure 8: Cross section of the RHIC proton-carbon polarimeter. A thin carbon ribbon target is passed across the beam (into page) and scattered carbon nuclei are measured in the six detectors.

Both of the RHIC hadron polarimeters can in principle be used for proton polarimetry at the EIC. At present two significant difficulties are foreseen. First, backgrounds in both polarimeters are observed and lie partially beneath the signal events. They are distinguished by timing distributions different from the signal allowing separation or estimation of a subtraction from the signal. At the EIC with higher bunch crossing frequency, the backgrounds will lie under the signal events from adjacent bunches and separation or subtraction based on timing will not be possible. Studies are under way to determine the nature of the background and possibly find a rejection method. Second, materials analysis of the carbon ribbon targets indicates that the the higher proton beam currents and bunch crossing frequencies at the EIC will induce heating to temperatures causing the targets to break after only a few seconds in the beam. A search for alternative target materials has been initiated.

A possible alternative to the pC polarimeter has been proposed. It is based on the observation by the PHENIX collaboration of a large azimuthal asymmetry of forward neutrons in the proton direction in p+Au collisions [**?**]. This effect is well described by a process of the high Z Au nucleus emitting a photon, which produces neutrons off of the polarized proton [**?**]. A polarimeter based on this process would replace the Au beam with a high Z fixed target as a source of photons; a Xe gas jet may be a suitable target. Such a polarimeter could be tested at RHIC in the final years of operation.

For light ion polarimetry at the EIC, the following methods can be considered:
– Using a polarized light ion jet target. Similarly to the proton beam measurement with hydrogen jet target, the light ion beam polarization is given by Eq. (7). Tagging of breakup of beam nuclei may be necessary to isolate the elastic scattering signal required for an absolute polarization measurement. However, a preliminary evaluation, based on deuterium beam scattering at HJET, indicates that the breakup contamination of the elastic data is small, only few percent, and, thus, the correction to Eq. (7) is expected to be negligible.
– Using polarized hydrogen jet target to measure light ion, e.g. He-3 (h), beam polarization. Since the beam and target particles are not identical, Eq. (7) should be corrected

$$P_{\text{beam}} = \frac{\epsilon_{\text{beam}}}{\epsilon_{\text{target}}} P_{\text{target}} \times \frac{\kappa_p - 2\text{Im}\, r_5^p - 2\text{Re}\, r_5^p\, T_R/T_c}{\kappa_h - 2\text{Im}\, r_5^h - 2\text{Re}\, r_5^h\, T_R/T_c} \tag{8}$$

where, $\kappa_p = \mu_p - 1 = 1.793$ and $\kappa_h = \mu_h/2 - 1/3 = -1.398$ are parameters derived from magnetic moments of proton and He-3, r_5^p and r_5^h are hadronic spin flip amplitudes [**?**] for $hp^\uparrow$ and $h^\uparrow p$ scattering, respectively, T_R is the recoil proton kinetic energy and $T_c = 4\pi\alpha Z_h/m_p\sigma_{\text{tot}}^{hp} \approx 0.7\,\text{MeV}$. Since $|r_5| = \mathcal{O}(1\%)$ are small, such measured absolute He-3 beam polarization will meet the EIC requirement if r_5^p and r_5^h can be related, with theoretical uncertainties better than 30–50%, to the proton-proton r_5 experimentally determined at HJET [**?**].
– Using low energy technique, e.g. [**?**], determine absolute light ion polarization in source and, than, monitor beam polarization decay and profile with beam acceleration control tools. This method is expected to work well if the beam polarization losses will be small at EIC. However, for a precision calibration, alternative measurements of the absolute polarization may be needed.

The pC polarimeter or an alternative developed for protons at the EIC should also provide suitable relative polarimetry for light ions.

The main polarimeters may be situated anywhere in the EIC hadron ring. The Hjet and pC polarimeters each require 1-2 m space along and transverse to the beam. However, one relative polarimeter (pC or alternative) should be placed near the experimental interaction point between the hadron spin rotators. The hadron polarimeters are only sensitive to transverse spin polarization. During longitudinal spin runs asymmetry measurements near the interaction point are required to verify that the transverse component of the spin direction is zero.

0.1.3 Luminosity Measurement:

The luminosity measurement provides the required normalization for all physics studies. At the broadest scale it determines absolute cross sections, such as needed for the structure function F_2 and derived PDFs. On an intermediate scale, it is also required to combine different running periods, such as runs with different beam energies needed to measure F_L, or runs with different beam species to study A dependencies. Asymmetry measurements are conducted using beams with bunches of both spin states. On the finest scale, the relative luminosity of the different bunch crossings is needed to normalize the event rates for the different states; the uncertainty on the relative bunch luminosity is a limiting factor for asymmetry measurements.

The bremsstrahlung process $e + p \longrightarrow e + p + \gamma$ was used successfully for the measurement of luminosity by the HERA collider experiments [**?**, **?**, **?**]. It has a precisely known QED cross-section which is large, minimizing theoretical uncertainty and providing negligible statistical uncertainty. Thus the scale uncertainty of the luminosity is determined by the systematic uncertainties of the counting of bremsstrahlung events. The ZEUS collaboration at HERA measured luminosity with a 1.7% scale uncertainty; further improvements at the EIC should be able to reduce this to $<1\%$ as required by the physics program.

In contrast to HERA, where only the electron beam was polarized, both the electron and proton/light ion beams will be polarized in the EIC. In this case the bremsstrahlung rate is sensitive to the polarization dependent term $a(P_e, P_h)$ in the cross section $\sigma_{\text{brems}} = \sigma_0(1 + a(P_e, P_h))$. Thus, the polarizations P_e, P_h and luminosity measurements are coupled, and the precision of the luminosity measurement is limited by the precision of the polarization measurement. This is especially important for relative luminosities for asymmetry measurements, where the bremsstrahlung process used for normalization has different cross sections for different spin states. The precision needed for the relative luminosity measurement is driven by the magnitude of the physics asymmetries which can be as low as 10^{-4}; the uncertainty on relative bunch luminosities must reach this level of precision.

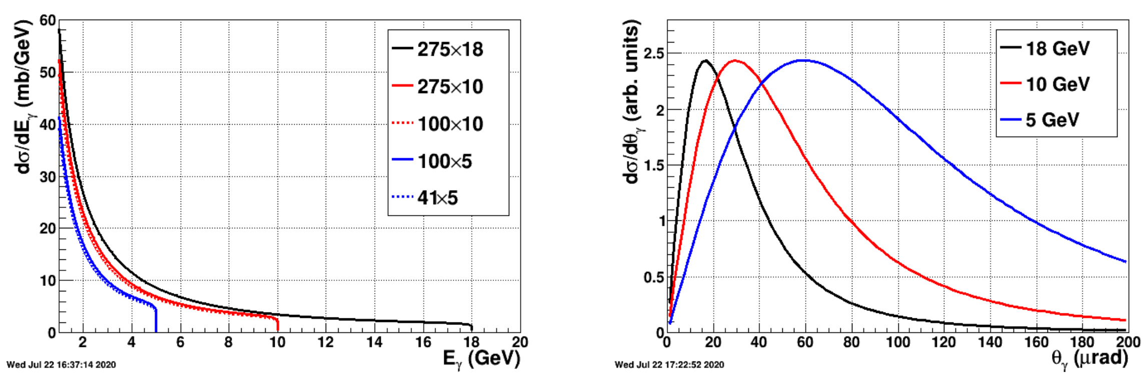

Figure 9: Bremsstrahlung photon energy (left) and angular (right) distributions for EIC beam energies.

The bremsstrahlung photon energy E_γ distributions for EIC beam energies are shown in the left of Fig. 9. They diverge as $E_g \to 0$ and have sharp cutoffs at the electron beam energies. As shown in the right of Fig. 9, the bremsstrahlung photons are strongly peaked in the forward direction with typical values of $\theta_\gamma \approx m_e/E_e$, with values of 20-60 μrad at the EIC. The RMS angular divergence of the electron beam is significantly larger than these values and will dominate the angular distribution of bremsstrahlung photons.

Far Backward Detectors: The path of the electron beam downstream of the interaction point is shown in Fig. 10. The horizontal axis is aligned with the direction of the beam at the collision point, along which photons from e+p and e+A interactions will travel. These photons come predominantly from the bremsstrahlung process used for luminosity determination. The lower left of the figure shows possible instrumentation for the luminosity measurement. Bremsstrahlung also produces electrons with momenta slightly below the beam energy. After being bent out of the beam by lattice dipoles they may be measured by taggers as shown in the top left of the figure.

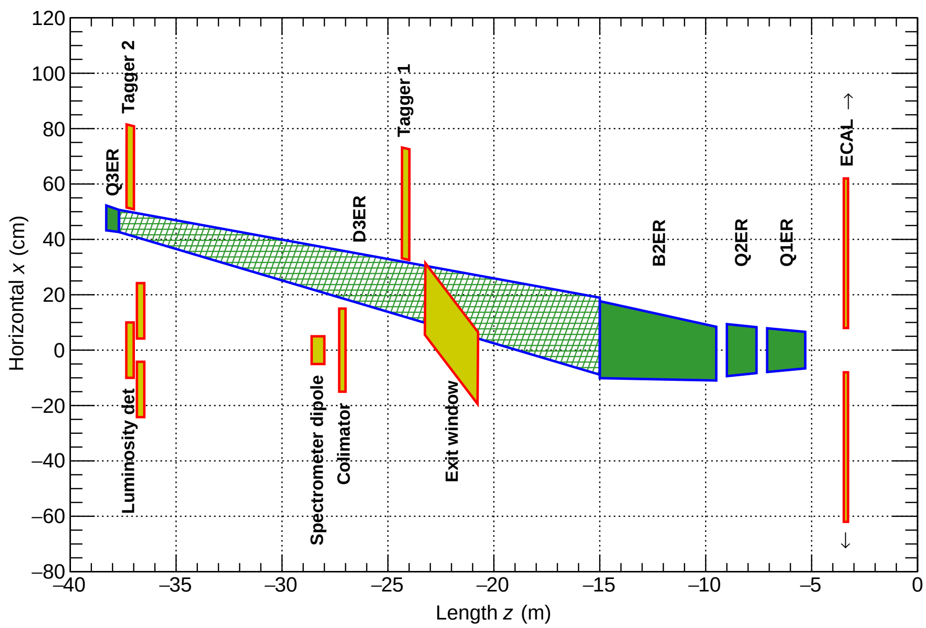

Figure 10: The region downstream of the interaction point in the electron direction.

Bremsstrahlung Photon Detectors: The straightforward method for measuring bremsstrahlung situates a calorimeter at zero degrees in the electron direction counting the resulting photons, as shown lower left of Fig. 10. The calorimeter is also exposed to the direct synchrotron radiation fan and must be shielded, thus degrading the energy resolution. This also imposes a rough low energy cutoff on photons typically $\approx$ 0.1-1 GeV below which the calorimeter is insensitive. At peak HERA luminosities, the photon calorimeters were sensitive to 1-2 photons per HERA bunch crossing. At an EIC luminosity of $10^{33}\,\text{cm}^{-2}\,\text{s}^{-1}$, the mean number of such photons per bunch crossing is over 20 for electron-proton scattering and increases with Z^2 of the target for nuclear beams. The per bunch energy distributions are broad, with a mean proportional to the number of photons per bunch crossing. The counting of bremsstrahlung photons thus is effectively an energy measurement in the photon calorimeter with all of the related systematic uncertainties (e.g. gain stability) of such a measurement.

An alternative method to counting bremsstrahlung photons, used effectively by the ZEUS collaboration at HERA, employs a pair spectrometer. A small fraction of photons is converted into e^+e^- pairs in the vacuum chamber exit window. A dipole magnet splits the pairs vertically and each particle hits a separate calorimeter adjacent to the unconverted photon path. The relevant components are depicted in the lower left of Fig. 10. This has several advantages over a zero-degree photon calorimeter:

- The calorimeters are outside of the primary synchrotron radiation fan.
- The exit window conversion fraction reduces the overall rate.
- The spectrometer geometry imposes a low energy cutoff in the photon spectrum, which depends on the magnitude of the dipole field and the location of the calorimeters.

The variable parameters of the last two points (conversion fraction, dipole field and calorimeter locations) may be chosen to reduce the rate to less than or of order one e^+e^- coincidence per bunch crossing even at nominal EIC luminosities. Thus, counting of bremsstrahlung photons is simply counting of e^+e^- coincidences in a pair spectrometer with only small corrections for pileup effects.

The locations of a zero-degree calorimeter and pair spectrometer are shown in the bottom left of Fig. 10. Careful integration into the machine lattice is required, not only to allow for enough space for the detectors, but also to accommodate the angular distribution of the photons. This is dominated by the angular divergence of the electron beam, with RMS values as high 0.2 mrad. Thus a clear aperture up to a few mrad is required to measure the angular distribution and minimize the acceptance correction. The spectrometer rate is directly proportional to the fraction of photons which convert into e^+e^- pairs, placing stringent requirements on the photon exit window. It must have a precisely known material composition, and a precisely measured and uniform thickness along the photon direction.

Calorimeters are required for both luminosity devices, for triggering and energy measurements. The high rates dictate a radiation hard design, especially for the zero-degree calorimeter, which must also have shielding against synchrotron radiation. The spectrometer must also have precise position detectors to measure the $e^{\pm}$. Combined with the calorimeter energy measurement this allows reconstruction of the converted photon positions. The distribution of photon positions is required to correct for the lost photons falling outside the photon aperture and detector acceptances.

Bremsstrahlung and Low-Q^2 Electron Detectors: Downstream of the interaction point the electron beam is accompanied by a flux of electrons at small angles with respect to the beam direction and at slightly lower energy. They are predominantly final state electrons from the bremsstrahlung process $e + p \longrightarrow e + p + \gamma$, with an energy distribution the mirror image of the left of Fig. 9 with $E'_e = E_e - E_\gamma$. Also, a fraction of the electrons in this region are produced in quasi-real photoproduction with $Q^2 \approx 0$.

The final state bremsstrahlung electrons provide a powerful tool for calibrating and verifying the luminosity measurement with photons. Tagging bremsstrahlung electrons and counting corresponding photons in the photon detectors provides a direct measure of the luminosity detector acceptance in the tagged energy range. This is of paramount importance to precisely determine the pair conversion probability for the luminosity spectrometer, which depends on the exit window composition and thickness.

Tagging of low-Q^2 processes provides an extension of the kinematic range of DIS processes measured with electrons in the central detector. It crosses the transition from DIS to hadronic reactions with quasi-real photons. An example of acceptance as a function of Q^2 for measurements with the central detector and electron taggers as depicted in Fig. 10 is shown in Fig. 11. The electrons are generated by a simple model of quasi-real photoproduction [**?**] and Pythia. The taggers provide useful acceptance in the range $10^{-6} < Q^2 < 10^{-2}$ GeV^2. Application of the electron taggers for low-Q^2 physics will face a challenge from the high rate bremsstrahlung electrons, which can be addressed by tagger design and correlation with information from the central detector.

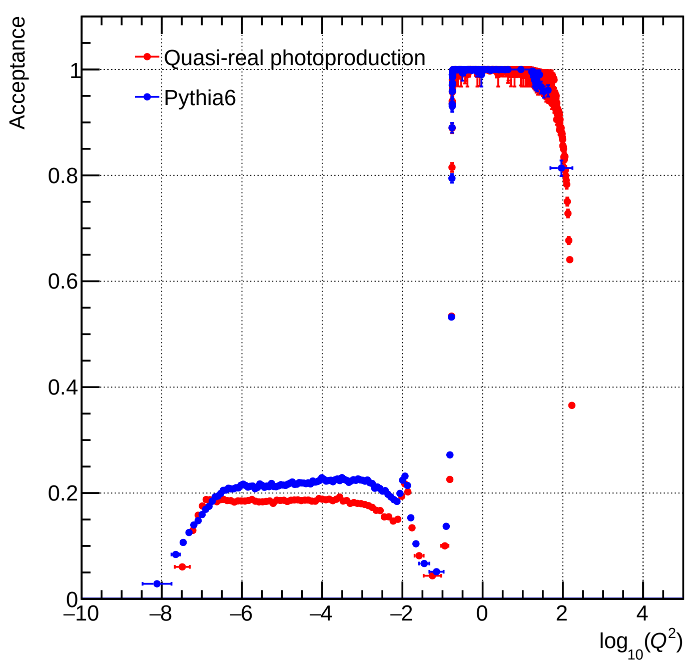

Figure 11: Acceptance as a function of Q^2 for electrons measured in the central detector (right plateau) and downstream taggers (left plateau). The electrons are generated by a simple model of quasi-real photoproduction and Pythia.

Possible locations of detectors for these electrons are shown in the top left of Fig. 10. Electrons with energies slightly below the beam are bent out of the beam by the first lattice dipole after the interaction point. The beam vacuum chamber must include exit windows for these electrons. The windows should be as thin as possible along the electron direction to minimize energy loss and multiple scattering before the detectors.

The taggers should include calorimeters for triggering and energy measurements. They should be finely segmented to disentangle the multiple electron hits per bunch crossing from the high rate bremsstrahlung process. The taggers should also have position sensitive detectors to measure the vertical and horizontal coordinates of electrons. The combined energy and position measurements allow reconstruction of the kinematic variable Q^2 and x_{BJ}. If the position detectors have multiple layers and are able to reconstruct the electron direction this will overconstrain the variable reconstruction and improve their measurement; this may also provide some measure of background rejection. The beam angular divergence will introduce significant errors on the variable reconstruction. The reconstructed versus generated Q^2 is shown in Fig. 12 with smearing from beam divergence. There is reasonable resolution for Q^2 as low as 10^{-3} GeV^2; below 10^{-4} GeV^2 meaningful reconstruction of Q^2 based on the electron is not possible.

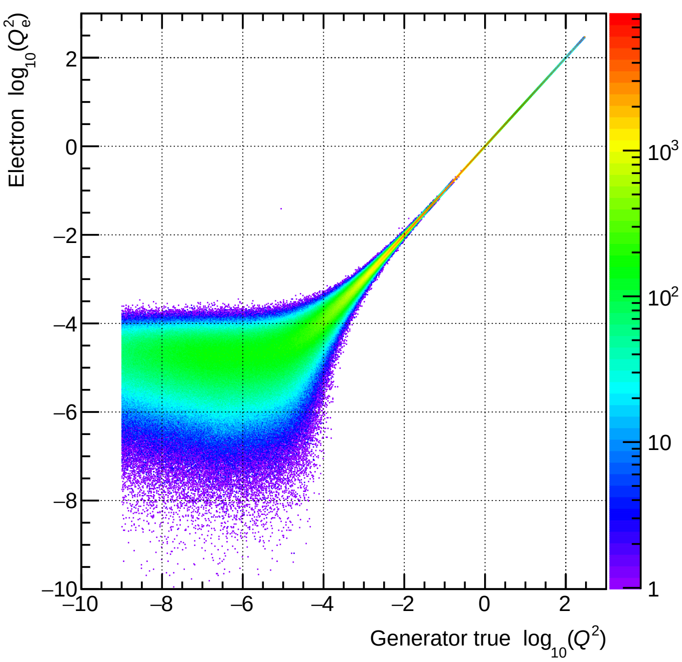

Figure 12: Comparison of reconstructed and reconstructed electron Q_e^2 with smearing for beam angular divergence.